PHYSICAL REVIEW A **88**, 012513 (2013)

Model operator approach to the Lamb shift calculations in relativistic many-electron atoms

V. M. Shabaev and I. I. Tupitsyn
Department of Physics, St. Petersburg State University, Ulianovskaya 1, Petrodvorets, St. Petersburg 198504, Russia

V. A. Yerokhin
Center for Advanced Studies, St. Petersburg State Polytechnical University, Polytekhnicheskaya 29, St. Petersburg 195251, Russia

(Received 27 May 2013; published 16 July 2013)

A model operator approach to calculations of the QED corrections to energy levels in relativistic many-electron atomic systems is developed. The model Lamb shift operator is represented by a sum of local and nonlocal potentials which are defined using the results of *ab initio* calculations of the diagonal and nondiagonal matrix elements of the one-loop QED operator with H-like wave functions. The model operator can be easily included in any calculations based on the Dirac-Coulomb-Breit Hamiltonian. The efficiency of the method is demonstrated by comparison of the model QED operator results for the Lamb shifts in many-electron atoms and ions with exact QED calculations.

DOI: 10.1103/PhysRevA.88.012513 PACS number(s): 31.30.J−, 12.20.Ds

I. INTRODUCTION

A good starting point for the relativistic atomic calculations is given by the Dirac-Coulomb-Breit (DCB) equation. This equation can be solved with high accuracy by using either the configuration-interaction Dirac-Fock (CI-DF) methods [1–7] or the relativistic many-body perturbation theory (RMBPT) methods [8–14]. In many cases the precision of these calculations has reached a level that requires evaluations of quantum electrodynamics (QED) effects. To date, the rigorous calculations of the QED effects in middle- and high-Z systems are fully restricted to the $1/Z$ perturbation theory (see, e.g., [15–19] and references therein). The perturbation theory methods have been also extended to many-electron ions and atoms employing an effective screening potential instead of the Coulomb one [20–27]. However, these methods are too complicated to be directly included in the DCB calculations. For this reason, numerous attempts have been undertaken to propose simple methods for incorporating the QED corrections in the CI-DF and RMBPT codes. These methods (see, e.g., [4,28–35] and references therein) are generally based on scaling the Lamb shift results for the Coulomb potential to other atomic potentials, which partially include the screening effects. Such a scaling can be done either directly by using Welton's idea [36] to express the main part of the self-energy contribution in terms of $\vec{\nabla}^2 V$ [4,29,34] or by introducing an effective short-range potential which fits the Lamb shifts for hydrogenlike ions [28,30–33,35].

In Ref. [37] it was shown that the QED corrections can be systematically included in an effective Hamiltonian acting in the space of the Slater determinants made up of one-electron positive-energy states whose total (many-electron) energies are smaller than the pair-creation threshold. To the lowest order, this approach leads to a QED operator that, in principle, can be added to the DCB Hamiltonian. The main goal of this paper is to represent this QED operator in a form that can be easily included in any calculations based on the DCB equation.

In the next section, we summarize the basic equations for the effective Hamiltonian that includes the one-loop QED corrections. Then we approximate the QED operator by a sum of short-range local and nonlocal potentials and calculate the model QED operator in a wide range of $Z = 10$–120. Finally, the model QED operator is applied to calculations of the Lamb shifts in many-electron atoms and ions, and the results obtained are compared with other QED calculations.

Relativistic units ($\hbar = c = 1$) are used throughout.

II. EFFECTIVE HAMILTONIAN IN THE FRAMEWORK OF QED

The systematic method to derive a Schrödinger-like equation for a relativistic many-electron atom from QED can be formulated within the two-time Green's function (TTGF) method [38]. To determine such an equation, first of all, one needs to choose the active space in which the effective Hamiltonian acts. Since rigorous calculations of the QED effects in middle- and high-Z systems employ the perturbation theory starting from the Dirac equation with a local potential, the active space is generally considered to be formed either by a single or by (quasi)degenerate unperturbed states. These states are given by the Slater determinants made up of the solutions of the Dirac equation with the local potential considered. However, in Ref. [37] it was shown that the active space can be extended to all unperturbed states made up of one-electron positive-energy states whose total (many-electron) energies are smaller than the pair-creation threshold. Moreover, if the consideration is restricted to the lowest-order QED terms, the active space can be extended beyond the pair-creation threshold. For simplicity, this extension, having no effect on the accuracy of the calculations, is considered in the present paper. Using the derivations presented in Ref. [37], we summarize below the basic equations that are obtained with this choice of the active space.

To simplify the equations, we assume that the active space is formed by the Slater determinants made up of the positive-energy solutions of the Dirac equation with the Coulomb potential $V_{\mathrm{C}}(r) = -\alpha Z_{\mathrm{nuc}}(r)/r$ [the effective charge $Z_{\mathrm{nuc}}(r)$ accounts for the nuclear charge distribution]:

$$h^{\mathrm{D}} \psi_n = \varepsilon_n \psi_n \,, \tag{1}$$

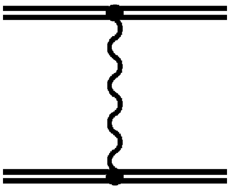

FIG. 1. One-photon exchange diagram.

where

$$h^{\rm D} = \vec{\alpha} \cdot \vec{p} + m\beta + V_{\rm C}(r) \tag{2}$$

is the one-electron Dirac Hamiltonian. We note, however, that all the equations can be easily adopted to the theory with the active space formed by the solutions in an effective potential $V_{\rm eff}(r)$ (e.g., the Dirac-Hartree, the Kohn-Sham, or a local version of the Dirac-Fock potential) that partly includes the screening effect. In this case, the interaction with the related counterterm $[V_{\rm C}(r) - V_{\rm eff}(r)]$ must be included in the total Hamiltonian. To construct the desired Hamiltonian, one should first consider the contribution from the one-photon exchange Feynman diagram (Fig. 1). Evaluation of this diagram with the TTGF method leads to the following symmetric form of the electron-electron interaction operator (for details see Refs. [37,38]):

$$\begin{aligned} h^{\rm int} = & \sum_{k\neq l, m\neq n}^{(\varepsilon_k,\varepsilon_l,\varepsilon_m,\varepsilon_n>0)} |\psi_k\psi_l\rangle\langle\psi_k\psi_l|\frac{1}{2}[I(\varepsilon_k-\varepsilon_m) \\ & + I(\varepsilon_l-\varepsilon_n)]|\psi_m\psi_n\rangle\langle\psi_m\psi_n|\,, \end{aligned} \tag{3}$$

where the indices k,l,m,n enumerate the positive-energy one-electron Dirac states, $|\psi_k\psi_l\rangle \equiv |\psi_k\rangle|\psi_l\rangle$ is the direct product of the one-electron Dirac wave functions $\psi_k(\vec{r}_1)$ and $\psi_l(\vec{r}_2)$,

$$I(\omega) = e^2\alpha_1^\rho\alpha_2^\sigma D_{\rho\sigma}(\omega,r_{12})\,, \tag{4}$$

$\alpha^\rho \equiv \gamma^0\gamma^\rho = (1,\boldsymbol{\alpha})$ are the Dirac matrices, $D_{\rho\sigma}(\omega,r_{12})$ is the photon propagator, and $r_{12} = |\vec{r}_1 - \vec{r}_2|$ is the interelectronic distance. It should be noted that the symmetric form of the frequency-dependent electron-electron interaction was first considered in Ref. [39]. The operator (3) defines the interaction between two electrons only. To get the total electron-electron interaction operator for a many-electron atom, one has to sum Eq. (3) over all pairs of atomic electrons:

$$H^{\rm int} = \sum_{i<j} h_{ij}^{\rm int}\,, \tag{5}$$

where $h_{ij}^{\rm int}$ is the two-electron operator (3) taken for electrons i and j.

Taking $D_{\rho\sigma}(\omega,r_{ij})$ in the Coulomb gauge at zero energy transfer ($\omega = 0$) leads to the Dirac-Coulomb-Breit Hamiltonian [40]:

$$H^{\rm DCB} = \Lambda^{(+)}\left[\sum_i h_i^{\rm D} + \sum_{i<j} V_{ij}\right]\Lambda^{(+)}\,, \tag{6}$$

where the indices i and j enumerate the atomic electrons, $\Lambda^{(+)}$ is the product of the one-electron projectors on the positive-energy states (which correspond to the potential $V_{\rm C}$), $h_i^{\rm D}$ is the one-electron Dirac Hamiltonian (2) taken for electron i,

FIG. 2. Self-energy diagram.

$$\begin{aligned} V_{ij} &= e^2\alpha_i^\rho\alpha_j^\sigma D_{\rho\sigma}(0,r_{ij}) = V_{ij}^{\rm C} + V_{ij}^{\rm B} \\ &= \frac{\alpha}{r_{ij}} - \alpha\left[\frac{\vec{\alpha}_i\cdot\vec{\alpha}_j}{r_{ij}} + \frac{1}{2}(\vec{\nabla}_i\cdot\vec{\alpha}_i)(\vec{\nabla}_j\cdot\vec{\alpha}_j)r_{ij}\right] \end{aligned} \tag{7}$$

is the sum of the Coulomb and Breit electron-electron interaction operators, and α is the fine-structure constant. It is well known that the DCB Hamiltonian accounts for the nonrelativistic and lowest-order relativistic contributions. In the Feynman gauge, to get the Hamiltonian to the same accuracy, one has to account for the higher-order photon exchange diagrams (see Ref. [37] and references therein).

As the next step, one should consider the contributions from the one-loop self-energy (SE) and vacuum-polarization (VP) diagrams presented in Figs. 2 and 3, respectively. The direct calculation of these contributions within the TTGF method leads to the following symmetric form of the one-electron QED operator $h^{\rm QED}$ [37]:

$$\begin{aligned} h^{\rm QED} = h^{\rm SE} + h^{\rm VP} = & \sum_{k,l}^{(\varepsilon_k,\varepsilon_l>0)} |\psi_k\rangle\langle\psi_k| \\ & \times \left\{\frac{1}{2}[\Sigma^{\rm SE}(\varepsilon_k) + \Sigma^{\rm SE}(\varepsilon_l)] + V^{\rm VP}\right\}|\psi_l\rangle\langle\psi_l|\,, \end{aligned} \tag{8}$$

where $\Sigma^{\rm SE}(\varepsilon_k)$ and $V^{\rm VP}$ are the renormalized SE and VP operators, respectively, and the sums over k and l go over all the positive-energy one-electron Dirac states. To get the total QED operator for a many-electron atom, one has to sum Eq. (8) over all atomic electrons:

$$\begin{aligned} H^{\rm QED} &= H^{\rm SE} + H^{\rm VP} \\ &= \sum_i h_i^{\rm QED} = \sum_i \left(h_i^{\rm SE} + h_i^{\rm VP}\right)\,, \end{aligned} \tag{9}$$

where $h_i^{\rm QED}$, $h_i^{\rm SE}$, and $h_i^{\rm VP}$ are the one-electron operators (8) taken for electron i.

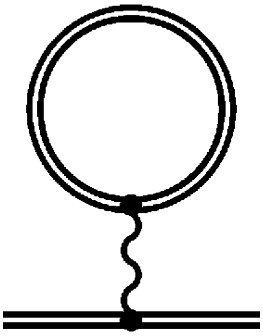

FIG. 3. Vacuum-polarization diagram.

Thus, within the lowest-order QED approximation the total effective Hamiltonian can be presented as

$$H = \Lambda^{(+)}\left[\sum_i \left(h_i^{\rm D} + h_i^{\rm QED}\right) + \sum_{i<j} h_{ij}^{\rm int}\right]\Lambda^{(+)}, \tag{10}$$

where the sums go over all atomic electrons and $h_{ij}^{\rm int}$, which is the two-electron operator (3) considered for electrons i and j, must be taken in the Coulomb gauge (if it is taken in the Feynman gauge, an additional term must be added to keep the same accuracy level [37]). In Eq. (10), all the operators are defined for the Coulomb potential $V_{\rm C}$. To get the corresponding Hamiltonian in the active space formed by the solutions in an effective potential $V_{\rm eff}$, one should do the evident replacements in all the operators, including the projector, and add the term $\Lambda^{(+)}\sum_i [V_{\rm C}(r_i) - V_{\rm eff}(r_i)]\Lambda^{(+)}$.

III. MODEL QED OPERATOR

Since the one-electron VP operator is given by the sum of the local Uehling and Wichmann-Kroll potentials [41], $V^{\rm VP} = V_{\rm Uehl} + V_{\rm WK}$, it can be easily included in the DCB equations. As is known, the dominant part of the VP contribution is represented by the Uehling potential:

$$V_{\rm Uehl}(r) = -\alpha Z \frac{2\alpha}{3\pi}\int_0^\infty dr'\, 4\pi r' \rho(r') \int_1^\infty dt \left(1 + \frac{1}{2t^2}\right) \times \frac{\sqrt{t^2-1}}{t^2}\, \frac{e^{(-2m|r-r'|t)} - e^{[-2m(r+r')t]}}{4mrt}, \tag{11}$$

where $Z\rho(r)$ is the density of the nuclear charge distribution $[\int \rho(r) d\mathbf{r} = 1]$. The Uehling potential can easily be evaluated by employing the approximate formulas from Ref. [42]. Including the screening effect in this potential causes no problem but hardly affects the result (see, e.g., Ref. [23]). Evaluation of the Wichmann-Kroll potential is a much more difficult problem [43–45]. However, to good accuracy, it can be calculated with the help of the approximate formulas derived in Ref. [46]. Therefore, in what follows, we restrict our consideration to the SE contribution only.

In principle, the operator $H^{\rm SE}$ defined by Eqs. (8) and (9) can be added to the DCB Hamiltonian to account for the lowest-order SE corrections. In practice, however, due to the absence of rather simple algorithms for the evaluation of the SE contributions for arbitrary states, we have to restrict $h^{\rm SE}$ to its matrix elements between a finite number of low-lying one-electron Dirac-Coulomb (or other effective potential) wave functions. This restriction strongly enlarges the interaction range of the SE operator and excludes highly excited bound and continuum spectrum components from the active space. As a result, such a potential may lead to the SE corrections which strongly deviate from the correct ones. For instance, in case of H-like ions it gives zero results for the states with the principal quantum number $n \geqslant 4$, provided the sums in (8) are limited by $n_k, n_l \leqslant 3$. To solve these problems, we modify the operator $h^{\rm SE}$ in two steps.

As the first step, to minimize the deviation of the representation (8), restricted to a finite number of states, from the exact one, we separate out a local (with respect to r) potential $V_{\rm loc}^{\rm SE}$ from the SE operator and employ formula (8) for the remaining SE part only. Such a separation can be justified by the fact that a dominant part of the nonrelativistic SE operator can be represented by a local short-range potential [36]. Due to the conservation of the angular quantum numbers by the one-electron SE operator, we can choose the local part to be different for different $\kappa = (-1)^{j+l+1/2}(j+1/2)$. With this in mind, we introduce the projector P_κ, which acts only on the angular variables and is defined by its kernel as

$$P_\kappa(\mathbf{n},\mathbf{n}') = \begin{pmatrix} \sum_m \Omega_{\kappa m}(\mathbf{n})\Omega^\dagger_{\kappa m}(\mathbf{n}') & 0 \\ 0 & \sum_m \Omega_{-\kappa m}(\mathbf{n})\Omega^\dagger_{-\kappa m}(\mathbf{n}') \end{pmatrix}, \tag{12}$$

where $\Omega_{\kappa m}(\mathbf{n})$ is a spherical spinor. Then, the local potential is given by

$$V_{\rm loc}^{\rm SE} = \sum_\kappa V_{{\rm loc},\kappa}^{\rm SE} P_\kappa\,, \tag{13}$$

where $V_{{\rm loc},\kappa}^{\rm SE}(r)$ is a short-range radial potential which can be chosen differently for different values of κ. Strictly speaking, the potential $V_{\rm loc}^{\rm SE}$ is semilocal. However, here and in what follows we label it as "local," keeping in mind that it is local only at a given value of κ. We put

$$V_{{\rm loc},\kappa}^{\rm SE}(r) = A_\kappa \exp\left(-r/\lambda_C\right), \tag{14}$$

where the constant A_κ is chosen to reproduce the SE shift for the lowest energy level at the given κ in the corresponding H-like ion and $\lambda_C = \hbar/(mc)$.

As the second step, we restrict the active space of the remaining SE operator, $h^{\rm SE} - V_{\rm loc}^{\rm SE}$, to the basis functions $\{\phi_i(\mathbf{r})\}_{i=1}^n$, which, having the same angular parts as the one-electron Dirac-Coulomb functions $\{\psi_i(\mathbf{r})\}_{i=1}^n$, are localized at smaller distances compared to the Dirac-Coulomb ones. The specific choice of the functions $\{\phi_i(\mathbf{r})\}_{i=1}^n$ will be given below. With these functions, we approximate the one-electron SE operator as follows:

$$h^{\rm SE} = V_{\rm loc}^{\rm SE} + \sum_{i,k=1}^n |\phi_i\rangle B_{ik} \langle\phi_k|\,, \tag{15}$$

where the matrix B_{ik} has to be determined in such a way that the matrix elements of the model SE operator (15) with the H-like wave functions, corresponding to the space under consideration, coincide with the exact ones. This leads to the equations

$$\sum_{j,l=1}^n \langle\psi_i|\phi_j\rangle B_{jl} \langle\phi_l|\psi_k\rangle = \langle\psi_i| \left\{\frac{1}{2}[\Sigma(\varepsilon_i) + \Sigma(\varepsilon_k)] - V_{\rm loc}^{\rm SE}\right\} |\psi_k\rangle\,. \tag{16}$$

Introducing the matrix $D_{ik} = \langle\phi_i|\psi_k\rangle$, we get

$$B_{ik} = \sum_{j,l=1}^n [(D^t)^{-1}]_{ij} \langle\psi_j| \left\{\frac{1}{2}[\Sigma(\varepsilon_j) + \Sigma(\varepsilon_l)] - V_{\rm loc}^{\rm SE}\right\} |\psi_l\rangle (D^{-1})_{lk}\,. \tag{17}$$

TABLE I. Self-energy correction for *ns* states, calculated with the hydrogenlike wave functions. Labels (n,n') denote the $F_{nn'}$ function defined by Eq. (24). R is the root-mean-square charge radius of the nucleus (in fermis). For each Z, the first line shows the point-nucleus result, whereas the second line displays the extended-nucleus result (if different).

Z	R	(1,1)	(1,2)	(1,3)	(1,4)	(1,5)	(2,2)	(2,3)	(2,4)	(2,5)	(3,3)	(3,4)	(3,5)	(4,4)	(4,5)	(5,5)
10	3.005	4.6542	4.7961	4.8145	4.8193	4.8210(1)	4.8944	4.9325	4.9437	4.9480	4.9524	4.9677	4.9740	4.9749	4.9824	4.9858
15	3.189	3.8014	3.9463	3.9639	3.9681	3.9693	4.0509	4.0885	4.0992	4.1030	4.1082	4.1229	4.1288	4.1296	4.1367	4.1396
		3.8013	3.9462	3.9639	3.9680	3.9693	4.0508	4.0885	4.0991	4.1030	4.1082	4.1229	4.1287	4.1296	4.1366	4.1396
20	3.476	3.2463	3.3946	3.4114	3.4148	3.4155	3.5066	3.5438	3.5538	3.5572	3.5633	3.5773	3.5826	3.5834	3.5899	3.5923
		3.2462	3.3945	3.4113	3.4147	3.4154	3.5065	3.5437	3.5537	3.5571	3.5632	3.5772	3.5825	3.5833	3.5898	3.5922
25	3.706	2.8501	3.0023	3.0183	3.0208	3.0209	3.1230	3.1597	3.1689	3.1716	3.1789	3.1922	3.1969	3.1975	3.2034	3.2052
		2.8499	3.0022	3.0182	3.0207	3.0207	3.1228	3.1595	3.1688	3.1715	3.1787	3.1920	3.1967	3.1974	3.2032	3.2050
30	3.929	2.5520	2.7087	2.7238	2.7253	2.7246	2.8388	2.8750	2.8835	2.8855	2.8940	2.9064	2.9105	2.9110	2.9162	2.9173
		2.5518	2.7084	2.7235	2.7251	2.7244	2.8386	2.8748	2.8832	2.8853	2.8937	2.9062	2.9102	2.9108	2.9159	2.9171
35	4.163	2.3200	2.4816	2.4958	2.4963	2.4949	2.6223	2.6580	2.6656	2.6669	2.6767	2.6882	2.6915	2.6919	2.6963	2.6967
		2.3196	2.4812	2.4954	2.4960	2.4945	2.6220	2.6576	2.6652	2.6665	2.6763	2.6878	2.6911	2.6915	2.6959	2.6963
40	4.270	2.1352	2.3024	2.3156	2.3151	2.3129	2.4548	2.4899	2.4965	2.4970	2.5083	2.5187	2.5213	2.5215	2.5250	2.5246
		2.1347	2.3019	2.3151	2.3146	2.3124	2.4543	2.4893	2.4960	2.4965	2.5078	2.5182	2.5208	2.5210	2.5245	2.5241
45	4.494	1.9859	2.1594	2.1716	2.1700	2.1668	2.3247	2.3591	2.3647	2.3643	2.3772	2.3865	2.3882	2.3882	2.3907	2.3894
		1.9853	2.1587	2.1709	2.1692	2.1661	2.3239	2.3583	2.3639	2.3635	2.3764	2.3857	2.3874	2.3874	2.3900	2.3887
50	4.654	1.8643	2.0448	2.0560	2.0531	2.0490	2.2243	2.2580	2.2625	2.2611	2.2757	2.2837	2.2844	2.2842	2.2857	2.2833
		1.8633	2.0438	2.0550	2.0521	2.0480	2.2233	2.2569	2.2614	2.2600	2.2747	2.2827	2.2834	2.2832	2.2846	2.2823
55	4.804	1.7648	1.9533	1.9635	1.9593	1.9542	2.1487	2.1816	2.1847	2.1822	2.1988	2.2054	2.2050	2.2045	2.2047	2.2012
		1.7635	1.9519	1.9621	1.9579	1.9527	2.1472	2.1800	2.1832	2.1807	2.1973	2.2039	2.2035	2.2030	2.2032	2.1997
60	4.912	1.6838	1.8815	1.8906	1.8848	1.8786	2.0945	2.1264	2.1281	2.1243	2.1431	2.1479	2.1463	2.1455	2.1443	2.1395
		1.6820	1.8795	1.8886	1.8829	1.8766	2.0923	2.1242	2.1259	2.1222	2.1410	2.1458	2.1442	2.1434	2.1422	2.1374
65	5.060	1.6186	1.8267	1.8346	1.8273	1.8197	2.0596	2.0904	2.0904	2.0852	2.1064	2.1092	2.1061	2.1049	2.1021	2.0958
		1.6161	1.8239	1.8318	1.8245	1.8169	2.0564	2.0872	2.0872	2.0821	2.1033	2.1061	2.1031	2.1019	2.0991	2.0928
70	5.311	1.5674	1.7876	1.7942	1.7850	1.7760	2.0429	2.0723	2.0703	2.0634	2.0874	2.0878	2.0831	2.0814	2.0767	2.0686
		1.5637	1.7833	1.7900	1.7808	1.7719	2.0381	2.0675	2.0655	2.0587	2.0826	2.0832	2.0785	2.0768	2.0721	2.0641
75	5.339	1.5290	1.7632	1.7683	1.7570	1.7464	2.0441	2.0718	2.0674	2.0586	2.0857	2.0834	2.0767	2.0744	2.0674	2.0573
		1.5239	1.7572	1.7624	1.7512	1.7406	2.0373	2.0650	2.0607	2.0519	2.0790	2.0767	2.0701	2.0678	2.0610	2.0509
80	5.463	1.5028	1.7533	1.7568	1.7431	1.7305	2.0639	2.0894	2.0822	2.0710	2.1018	2.0961	2.0870	2.0840	2.0744	2.0619
		1.4955	1.7447	1.7482	1.7346	1.7221	2.0537	2.0793	2.0722	2.0611	2.0917	2.0862	2.0772	2.0743	2.0648	2.0524
85	5.539	1.4888	1.7587	1.7602	1.7435	1.7287	2.1039	2.1266	2.1158	2.1018	2.1369	2.1271	2.1152	2.1113	2.0985	2.0831
		1.4784	1.7461	1.7477	1.7312	1.7165	2.0886	2.1115	2.1009	2.0871	2.1219	2.1124	2.1006	2.0968	2.0842	2.0689
90	5.710	1.4875	1.7806	1.7797	1.7595	1.7420	2.1669	2.1860	2.1708	2.1533	2.1936	2.1786	2.1631	2.1582	2.1415	2.1225
		1.4721	1.7615	1.7607	1.7408	1.7236	2.1431	2.1625	2.1477	2.1305	2.1702	2.1557	2.1406	2.1357	2.1194	2.1007
95	5.905	1.5005	1.8218	1.8176	1.7931	1.7723	2.2575	2.2719	2.2510	2.2291	2.2757	2.2543	2.2344	2.2280	2.2066	2.1831
		1.4772	1.7921	1.7882	1.7642	1.7439	2.2197	2.2345	2.2143	2.1929	2.2386	2.2180	2.1987	2.1925(1)	2.1717	2.1488
100	5.857	1.5302	1.8863	1.8779	1.8479	1.8230	2.3831	2.3910	2.3627	2.3351	2.3897	2.3600	2.3343	2.3262	2.2987	2.2697
		1.4961	1.8417	1.8338	1.8047	1.7806	2.3247	2.3332	2.3061	2.2795	2.3325	2.3042	2.2795	2.2717(1)	2.2453(1)	2.2172
105	5.919	1.5809	1.9811	1.9670	1.9298	1.8996	2.5553	2.5543	2.5158	2.4807	2.5457	2.5051	2.4718	2.4615	2.4261	2.3899
		1.5286	1.9107	1.8974	1.8619	1.8331	2.4602	2.4604	2.4243	2.3911	2.4531	2.4150	2.3836	2.3737	2.3403(1)	2.3058
110	5.993	1.6601	2.1179	2.0956	2.0487	2.0114	2.7936	2.7797	2.7272	2.6819	2.7609	2.7055	2.6617	2.6484	2.6025	2.5566
		1.5771	2.0031	1.9824	1.9388	1.9040	2.6334	2.6222	2.5743	2.5325	2.6058	2.5552	2.5151	2.5026(1)	2.4604(2)	2.4179
115	6.088	1.7811	2.3180	2.2832	2.2224	2.1751	3.1331	3.1001	3.0270	2.9668	3.0659	2.9893	2.9307	2.9131	2.8527	2.7933
		1.6441	2.1228	2.0917	2.0375	1.9952	2.8519	2.8248	2.7610	2.7081	2.7958	2.7288	2.6775	2.6617(1)	2.6084(1)	2.5556
120	6.175	1.9709	2.6233	2.5685	2.4866(1)	2.4243(1)	3.6437	3.5804(1)	3.4750(1)	3.3921(1)	3.5219(1)	3.4131	3.3319	3.3080	3.2259	3.1464
		1.7335(1)	2.2753(1)	2.2294(1)	2.1613(1)	2.1093(1)	3.1256(1)	3.0760(1)	2.9909(1)	2.9231(1)	3.0295(1)	2.9411(1)	2.8750(1)	2.8549(2)	2.7875(1)	2.7216

Therefore, the model one-electron SE operator can be written as

$$h^{\rm SE} = V^{\rm SE}_{\rm loc} + \sum_{i,k=1}^{n}\sum_{j,l=1}^{n} |\phi_i\rangle[(D^t)^{-1}]_{ij} \times\langle\psi_j|\left\{\frac{1}{2}[\Sigma(\varepsilon_j)+\Sigma(\varepsilon_l)] - V^{\rm SE}_{\rm loc}\right\}|\psi_l\rangle \times(D^{-1})_{lk}\langle\phi_k|\,. \qquad (18)$$

Now let us consider the choice of the functions $\{\phi_i(\mathbf{r})\}_{i=1}^{n}$. On the one hand, since we use the SE matrix elements calculated with the hydrogenlike wave functions, these functions should be chosen rather close to the H-like ones. On the other hand, because of a short interaction range of the SE operator, they should vanish at smaller distances compared to the H-like wave functions. With this in mind, we construct them using the H-like wave functions multiplied by the factor

$$\rho_l(r) = \exp\left[-2\alpha Z(r/\bar{\lambda}_C)/(1+l)\right], \qquad (19)$$

where $l = |\kappa + 1/2| - 1/2$ is the orbital angular momentum of the state under consideration. The simple choice $\phi_i(\mathbf{r}) = \rho_{l_i}(r)\psi_i(\mathbf{r})$ fits the goal but, due to a rather similar behavior of the wave functions for different values of the principal quantum number at small r, gives a matrix D close to the degenerate one and therefore leads to a rather singular matrix D^{-1}. For this reason, we consider a slightly different choice. In what follows, we restrict the basis functions to ns, $np_{1/2}$, $np_{3/2}$, $nd_{3/2}$, and $nd_{5/2}$ states with the principal quantum number $n \leqslant 3$ for the s states and $n \leqslant 4$ for the p and d states and put

$$\phi_i(\mathbf{r}) = \tfrac{1}{2}[I - (-1)^{s_i}\beta]\rho_{l_i}(r)\psi_i(\mathbf{r})\,, \qquad (20)$$

where I is the identity matrix, β is the standard Dirac matrix, the index $s_i = n_i - l_i$ enumerates the positive energy states at

TABLE II. Self-energy correction for $np_{1/2}$ states, calculated with the hydrogenlike wave functions.

Z	R	(2,2)	(2,3)	(2,4)	(2,5)	(3,3)	(3,4)	(3,5)	(4,4)	(4,5)	(5,5)
10	3.005	−0.1148	−0.0962	−0.0946	−0.0946	−0.1020	−0.0941	−0.0923	−0.0964(1)	−0.0921	−0.0932
15	3.189	−0.1045	−0.0851	−0.0833	−0.0831	−0.0901	−0.0818	−0.0799	−0.0837	−0.0794	−0.0803
20	3.476	−0.0925	−0.0721	−0.0699	−0.0696	−0.0760	−0.0674	−0.0653	−0.0690	−0.0644	−0.0653
25	3.706	−0.0791	−0.0576	−0.0550	−0.0545	−0.0603	−0.0512	−0.0489	−0.0525	−0.0477	−0.0484
30	3.929	−0.0643	−0.0416	−0.0386	−0.0379	−0.0431	−0.0336	−0.0310	−0.0344	−0.0295	−0.0299
35	4.163	−0.0483	−0.0242	−0.0207	−0.0199	−0.0244	−0.0144	−0.0116	−0.0148	−0.0097	−0.0099
40	4.270	−0.0310	−0.0054	−0.0014	−0.0003	−0.0042	0.0063	0.0094	0.0063	0.0117	0.0116
45	4.494	−0.0123	0.0150	0.0196	0.0208	0.0177	0.0287	0.0321	0.0291	0.0347	0.0347
50	4.654	0.0080	0.0371	0.0423	0.0438	0.0414	0.0529	0.0566	0.0538	0.0595	0.0597
55	4.804	0.0303	0.0614	0.0672	0.0689	0.0672	0.0793	0.0833	0.0805	0.0864	0.0867
60	4.912	0.0548	0.0881	0.0946	0.0965	0.0956	0.1083	0.1125	0.1098	0.1158	0.1161
		0.0547	0.0881	0.0946	0.0965	0.0955	0.1082	0.1125	0.1098	0.1157	0.1161
65	5.060	0.0820	0.1178	0.1250	0.1271	0.1271	0.1402	0.1448	0.1421	0.1481	0.1485
		0.0819	0.1177	0.1249	0.1270	0.1270	0.1401	0.1447	0.1420	0.1480	0.1484
70	5.311	0.1127	0.1512	0.1591	0.1614	0.1623	0.1760	0.1807	0.1781	0.1840	0.1844
		0.1126	0.1510	0.1590	0.1612	0.1621	0.1758	0.1805	0.1778	0.1838	0.1841
75	5.339	0.1477	0.1891	0.1979	0.2002	0.2023	0.2164	0.2213	0.2186	0.2244	0.2246
		0.1474	0.1888	0.1975	0.1999	0.2020	0.2160	0.2209	0.2182	0.2240	0.2242
80	5.463	0.1882	0.2329	0.2424	0.2448	0.2483	0.2626	0.2677	0.2649	0.2704	0.2703
		0.1877	0.2323	0.2418	0.2441	0.2476	0.2619	0.2670	0.2642	0.2697	0.2696
85	5.539	0.2359	0.2843	0.2944	0.2967	0.3020	0.3165	0.3215	0.3185	0.3236	0.3230
		0.2349	0.2832	0.2933	0.2955	0.3008	0.3152	0.3202	0.3173	0.3223	0.3217
90	5.710	0.2931	0.3457	0.3563	0.3583	0.3660	0.3803	0.3850	0.3819	0.3862	0.3849
		0.2912	0.3436	0.3542	0.3562	0.3637	0.3780	0.3827	0.3795	0.3838	0.3825
95	5.905	0.3633	0.4205	0.4315	0.4329	0.4438	0.4575	0.4616	0.4583	0.4613	0.4589
		0.3597	0.4166	0.4275	0.4288	0.4394	0.4531	0.4572	0.4538	0.4569	0.4544
100	5.857	0.4517	0.5143	0.5251	0.5254	0.5408	0.5533	0.5563	0.5525	0.5538	0.5498
		0.4450	0.5070	0.5177	0.5180	0.5327	0.5452	0.5482	0.5443	0.5456	0.5416
105	5.919	0.5669	0.6355	0.6454	0.6438	0.6655	0.6758	0.6768	0.6725	0.6711	0.6645
		0.5537	0.6211	0.6308	0.6294	0.6498	0.6600	0.6610	0.6566	0.6552	0.6487
110	5.993	0.7231	0.7984	0.8059	0.8012	0.8322	0.8385	0.8361	0.8311	0.8254	0.8150
		0.6961	0.7689	0.7763	0.7719	0.8002	0.8064	0.8043	0.7989(1)	0.7936	0.7834
115	6.088	0.9468	1.0292	1.0314	1.0212	1.0668	1.0659	1.0575	1.0513	1.0388	1.0222
		0.8881	0.9656	0.9681	0.9587	0.9983	0.9977	0.9902	0.9834(1)	0.9719(1)	0.9561
120	6.175	1.2926	1.3816	1.3726	1.3522	1.4219	1.4074	1.3881	1.3798	1.3557	1.3286
		1.1559	1.2352	1.2280	1.2102	1.2658	1.2532(1)	1.2369(1)	1.2275(2)	1.2064(2)	1.1819

the given κ, and n_i is the principal quantum number. With this choice, one easily finds

$$
\begin{aligned}
D_{11} &= \int_0^\infty dr\, r^2 g_1^2(r)\, \rho_l(r)\,, \\
D_{12} &= \int_0^\infty dr\, r^2 g_1(r)\, g_2(r)\, \rho_l(r)\,, \\
D_{13} = D_{31} &= \int_0^\infty dr\, r^2 g_1(r)\, g_3(r)\, \rho_l(r)\,, \\
D_{21} &= \int_0^\infty dr\, r^2 f_1(r)\, f_2(r)\, \rho_l(r)\,, \\
D_{22} &= \int_0^\infty dr\, r^2 f_2^2(r)\, \rho_l(r)\,, \\
D_{23} &= \int_0^\infty dr\, r^2 f_2(r)\, f_3(r)\, \rho_l(r)\,, \\
D_{32} &= \int_0^\infty dr\, r^2 g_2(r)\, g_3(r)\, \rho_l(r)\,, \\
D_{33} &= \int_0^\infty dr\, r^2 g_3^2(r)\, \rho_l(r)\,,
\end{aligned}
\tag{21}
$$

where $g_i(r)$ and $f_i(r)$ are the upper and lower radial components of the hydrogenlike wave functions and index i enumerates the positive-energy states at the given κ. The explicit formulas for the calculation of the inverse matrix can be found in standard textbooks.

Thus, in what follows we use the model one-electron SE operator given by

$$
\begin{aligned}
h^{\rm SE} = V_{\rm loc}^{\rm SE} &+ \frac{1}{4}\sum_{i,k}\sum_{j,l}[I-(-1)^{s_i}\beta]\rho_{l_i}(r)|\psi_i\rangle \\
&\times[(D^t)^{-1}]_{ij}\langle\psi_j|\left\{\frac{1}{2}[\Sigma(\varepsilon_j)+\Sigma(\varepsilon_l)]-V_{\rm loc}^{\rm SE}\right\}|\psi_l\rangle \\
&\times(D^{-1})_{lk}\langle\psi_k|\rho_{l_k}(r)[I-(-1)^{s_k}\beta],
\end{aligned}
\tag{22}
$$

TABLE III. Self-energy correction for $np_{3/2}$ states, calculated with the hydrogenlike wave functions.

Z	R	(2,2)	(2,3)	(2,4)	(2,5)	(3,3)	(3,4)	(3,5)	(4,4)	(4,5)	(5,5)
10	3.005	0.1304	0.1335	0.1316	0.1301	0.1421	0.1454	0.1457	0.1474	0.1496	0.1503
15	3.189	0.1366	0.1399	0.1380	0.1365	0.1490	0.1525	0.1527	0.1546	0.1569	0.1576
20	3.476	0.1438	0.1473	0.1455	0.1440	0.1572	0.1607	0.1610	0.1630	0.1654	0.1662
25	3.706	0.1519	0.1556	0.1537	0.1523	0.1663	0.1699	0.1702	0.1725	0.1749	0.1758
30	3.929	0.1606	0.1646	0.1627	0.1612	0.1761	0.1799	0.1803	0.1827	0.1852	0.1861
35	4.163	0.1699	0.1741	0.1722	0.1706	0.1866	0.1906	0.1909	0.1936	0.1962	0.1972
40	4.270	0.1796	0.1841	0.1821	0.1805	0.1977	0.2019	0.2022	0.2052	0.2078	0.2090
45	4.494	0.1897	0.1945	0.1925	0.1908	0.2093	0.2137	0.2140	0.2173	0.2200	0.2213
50	4.654	0.2001	0.2053	0.2032	0.2015	0.2214	0.2260	0.2264	0.2299	0.2328	0.2341
55	4.804	0.2107	0.2165	0.2143	0.2124	0.2340	0.2388	0.2392	0.2431	0.2461	0.2475
60	4.912	0.2216	0.2279	0.2256	0.2237	0.2471	0.2521	0.2525	0.2568	0.2599	0.2615
65	5.060	0.2328	0.2397	0.2373	0.2353	0.2605	0.2660	0.2663	0.2710	0.2743	0.2760
70	5.311	0.2441	0.2517	0.2493	0.2472	0.2745	0.2803	0.2807	0.2858	0.2892	0.2910
75	5.339	0.2556	0.2641	0.2616	0.2594	0.2889	0.2951	0.2955	0.3011	0.3047	0.3067
		0.2555	0.2640	0.2615	0.2593	0.2888	0.2950	0.2954	0.3010	0.3046	0.3066
80	5.463	0.2672	0.2767	0.2742	0.2718	0.3038	0.3105	0.3109	0.3171	0.3208	0.3230
		0.2671	0.2766	0.2741	0.2717	0.3036	0.3103	0.3107	0.3169	0.3207	0.3228
85	5.539	0.2789	0.2896	0.2871	0.2846	0.3191	0.3264	0.3269	0.3336	0.3376	0.3399
		0.2787	0.2894	0.2869	0.2844	0.3189	0.3261	0.3266	0.3333	0.3373	0.3396
90	5.710	0.2907	0.3028	0.3003	0.2977	0.3350	0.3428	0.3434	0.3507	0.3550	0.3575
		0.2904	0.3024	0.3000	0.2973	0.3346	0.3424	0.3430	0.3503	0.3545	0.3570
95	5.905	0.3024	0.3161	0.3138	0.3111	0.3512	0.3598	0.3605	0.3685	0.3730	0.3757
		0.3020	0.3156	0.3132	0.3105	0.3506	0.3592	0.3598	0.3678	0.3723	0.3750
100	5.857	0.3141	0.3297	0.3275	0.3247	0.3679	0.3773	0.3781	0.3868	0.3917	0.3946
		0.3135	0.3289	0.3267	0.3239	0.3670	0.3764	0.3771	0.3858	0.3906	0.3935
105	5.919	0.3256	0.3433	0.3414	0.3385	0.3849	0.3953	0.3963	0.4056	0.4109	0.4140
		0.3248(1)	0.3421	0.3402	0.3373	0.3836	0.3938	0.3948	0.4041	0.4093	0.4124
110	5.993	0.3368	0.3567	0.3552	0.3523	0.4020	0.4134	0.4146	0.4247	0.4304	0.4338
		0.3356(1)	0.3552	0.3535	0.3506	0.4002	0.4113	0.4125	0.4225	0.4281	0.4315
115	6.088	0.3473	0.3698	0.3688	0.3660	0.4189	0.4314	0.4329	0.4437	0.4498	0.4535(1)
		0.3457(1)	0.3676	0.3665	0.3635	0.4163	0.4285	0.4300	0.4407	0.4467	0.4502(1)
120	6.175	0.3567	0.3819	0.3816	0.3789	0.4348	0.4484	0.4504	0.4617	0.4683	0.4722(1)
		0.3548(1)	0.3792	0.3786	0.3757	0.4316(1)	0.4448	0.4466	0.4580	0.4643	0.4681(1)

where the summations run over ns states with the principal quantum number $n \leqslant 3$ and over $np_{1/2}$, $np_{3/2}nd_{3/2}$, and $nd_{5/2}$ states with $n \leqslant 4$, $\rho_{l_i}(r) = \exp\left[-2\alpha Z(r/\lambda_C)/(1+l_i)\right]$,

$$D_{ik} = \tfrac{1}{2}\langle\psi_i|[I - (-1)^{s_i}\beta]\rho_{l_i}(r)|\psi_k\rangle\,, \qquad (23)$$

and $V^{\rm SE}_{\rm loc}$ is defined by Eqs. (13) and (14).

IV. MATRIX ELEMENTS OF THE EXACT SELF-ENERGY OPERATOR

To complete our construction of the model SE operator, we need the diagonal and nondiagonal matrix elements of the exact SE operator $\Sigma(\varepsilon)$ with the hydrogenlike wave functions. Calculations of the SE corrections reported previously in the literature [47–49] were performed for the diagonal matrix elements only. In the present work, we extend these calculations to both the diagonal and nondiagonal matrix elements of the one-loop SE operator. Our calculation was carried out in two steps. First, we evaluated the SE matrix element for the point nucleus by using the numerical method described in detail in Refs. [50,51]. Next, we separately calculated the finite nuclear size correction, as described in Ref. [52]. The finite nuclear size effect was calculated with the standard two-parameter Fermi model for the nuclear charge distribution.

The results of our calculations for the ns, $np_{1/2}$, $np_{3/2}$, $nd_{3/2}$, and $nd_{5/2}$ states with n up to 5 are presented in Tables I, II, III, IV, and V, respectively. They are expressed in terms of the function $F_{ik}(\alpha Z)$, defined by

$$\begin{aligned}\Sigma_{ik} &\equiv \langle\psi_i|\frac{1}{2}[\Sigma(\varepsilon_i) + \Sigma(\varepsilon_k)]|\psi_k\rangle \\ &= \frac{\alpha}{\pi}\frac{(\alpha Z)^4}{(n_i n_k)^{3/2}}F_{ik}(\alpha Z)mc^2\,, \end{aligned} \qquad (24)$$

where n_i and n_k are the principal quantum numbers of the i and k states, respectively. In the tables, the results are presented separately for the point nucleus and for the extended nucleus (except for the cases when both results coincide). If no error is specified, the results are supposed to be accurate to all digits quoted. In the case of diagonal matrix elements, excellent agreement with previous results [47–49] is observed. In this paper, to define the model SE operator we use the values $F_{ik}(\alpha Z)$ with the principal quantum numbers $n_i, n_k \leqslant 3$ for the s states and $n_i, n_k \leqslant 4$ for the p and d states. As for the other data presented in the tables, they can be used for test

TABLE IV. Self-energy correction for $nd_{3/2}$ states, calculated with the hydrogenlike wave functions.

Z	R	(3,3)	(3,4)	(3,5)	(4,4)	(4,5)	(5,5)
10	3.005	−0.0427(1)	−0.0352	−0.0344(1)	−0.0407	−0.0371	−0.0395(1)
15	3.189	−0.0424	−0.0349	−0.0341	−0.0403	−0.0368	−0.0391
20	3.476	−0.0420	−0.0345	−0.0337	−0.0399	−0.0363	−0.0387
25	3.706	−0.0415	−0.0340	−0.0332	−0.0393	−0.0358	−0.0381
30	3.929	−0.0410	−0.0334	−0.0327	−0.0387	−0.0351	−0.0374
35	4.163	−0.0404	−0.0328	−0.0320	−0.0379	−0.0343	−0.0366
40	4.270	−0.0396	−0.0320	−0.0313	−0.0371	−0.0334	−0.0356
45	4.494	−0.0388	−0.0310	−0.0304	−0.0360	−0.0323	−0.0345
50	4.654	−0.0378	−0.0300	−0.0293	−0.0348	−0.0310	−0.0331
55	4.804	−0.0366	−0.0287	−0.0280	−0.0334	−0.0295	−0.0316
60	4.912	−0.0353	−0.0272	−0.0266	−0.0317	−0.0277	−0.0298
65	5.060	−0.0338	−0.0255	−0.0249	−0.0298	−0.0257	−0.0276
70	5.311	−0.0321	−0.0236	−0.0229	−0.0276	−0.0233	−0.0252
75	5.339	−0.0302	−0.0213	−0.0206	−0.0251	−0.0206	−0.0223
80	5.463	−0.0279	−0.0187	−0.0180	−0.0221	−0.0174	−0.0190
85	5.539	−0.0254	−0.0157	−0.0149	−0.0188	−0.0137	−0.0152
90	5.710	−0.0225	−0.0123	−0.0114	−0.0149	−0.0095	−0.0108
95	5.905	−0.0192	−0.0083	−0.0073	−0.0104	−0.0046	−0.0058
100	5.857	−0.0154	−0.0037	−0.0026	−0.0053	0.0010	0.0001
105	5.919	−0.0111	0.0015	0.0029	0.0006	0.0074	0.0068
		−0.0112	0.0014	0.0028	0.0005	0.0073	0.0067
110	5.993	−0.0062	0.0074	0.0091	0.0074	0.0148	0.0145
		−0.0063	0.0073	0.0090	0.0072	0.0146	0.0143
115	6.088	−0.0007	0.0142	0.0163	0.0151	0.0232	0.0232
		−0.0009	0.0139	0.0160	0.0148	0.0229	0.0229
120	6.175	0.0055	0.0219	0.0245	0.0238	0.0328	0.0332(1)
		0.0051(1)	0.0214	0.0239	0.0232	0.0321	0.0324(1)

TABLE V. Self-energy correction for $nd_{5/2}$ states, calculated with the hydrogenlike wave functions.

Z	R	(3,3)	(3,4)	(3,5)	(4,4)	(4,5)	(5,5)
10	3.005	0.0408	0.0377	0.0354	0.0428	0.0424	0.0440
15	3.189	0.0412	0.0381	0.0358	0.0433	0.0429	0.0445
20	3.476	0.0417	0.0386	0.0363	0.0440	0.0435	0.0452
25	3.706	0.0424	0.0393	0.0370	0.0448	0.0443	0.0460
30	3.929	0.0432	0.0401	0.0377	0.0457	0.0453	0.0470
35	4.163	0.0441	0.0410	0.0386	0.0467	0.0463	0.0481
40	4.270	0.0452	0.0420	0.0396	0.0479	0.0475	0.0494
45	4.494	0.0463	0.0431	0.0407	0.0493	0.0489	0.0508
50	4.654	0.0475	0.0443	0.0419	0.0507	0.0504	0.0524
55	4.804	0.0489	0.0457	0.0432	0.0523	0.0520	0.0542
60	4.912	0.0503	0.0472	0.0446	0.0541	0.0538	0.0560
65	5.060	0.0519	0.0487	0.0462	0.0560	0.0557	0.0581
70	5.311	0.0536	0.0504	0.0478	0.0580	0.0578	0.0602
75	5.339	0.0553	0.0522	0.0496	0.0601	0.0600	0.0626
80	5.463	0.0572	0.0541	0.0514	0.0624	0.0623	0.0650
85	5.539	0.0591	0.0561	0.0534	0.0648	0.0647	0.0676
90	5.710	0.0612	0.0582	0.0554	0.0673	0.0673	0.0704
95	5.905	0.0633	0.0603	0.0575	0.0700	0.0700	0.0732
100	5.857	0.0654	0.0626	0.0597	0.0727	0.0728	0.0762
105	5.919	0.0677	0.0648	0.0619	0.0755	0.0757	0.0792
110	5.993	0.0699	0.0672	0.0642	0.0783	0.0786	0.0824
115	6.088	0.0722	0.0695	0.0665	0.0812	0.0816	0.0855(1)
120	6.175	0.0745	0.0719	0.0688	0.0841	0.0846	0.0887(1)

TABLE VI. The self-energy function $F(\alpha Z)$, defined by $\Delta E^{\rm SE} = \frac{\alpha}{\pi}\frac{(\alpha Z)^4}{n^3}F(\alpha Z)mc^2$, for H-like ions. $\langle v|h^{\rm SE}|v\rangle$ denotes the results of the model SE operator approach, $\langle v|V^{\rm SE}_{\rm loc}|v\rangle$ is the contribution of the local part of the model SE operator, and "Exact" labels the results of the exact calculation.

Z	State	$\langle v\|V^{\rm SE}_{\rm loc}\|v\rangle$	$\langle v\|h^{\rm SE}\|v\rangle$	Exact
10	$4s$	4.60	4.96	4.97
	$5s$	4.59	4.96	4.99
	$5p_{1/2}$	−0.15	−0.10	−0.09
	$5p_{3/2}$	0.17	0.15	0.15
	$5d_{3/2}$	−0.07	−0.05	−0.04
	$5d_{5/2}$	0.07	0.05	0.04
20	$4s$	3.11	3.57	3.58
	$5s$	3.11	3.57	3.59
	$5p_{1/2}$	−0.12	−0.08	−0.07
	$5p_{3/2}$	0.18	0.16	0.17
	$5d_{3/2}$	−0.07	−0.05	−0.04
	$5d_{5/2}$	0.07	0.05	0.05
40	$4s$	1.91	2.51	2.52
	$5s$	1.90	2.50	2.52
	$5p_{1/2}$	−0.04	0.00	0.01
	$5p_{3/2}$	0.22	0.21	0.21
	$5d_{3/2}$	−0.06	−0.04	−0.04
	$5d_{5/2}$	0.07	0.06	0.05
60	$4s$	1.46	2.13	2.14
	$5s$	1.44	2.12	2.14
	$5p_{1/2}$	0.06	0.11	0.12
	$5p_{3/2}$	0.26	0.26	0.26
	$5d_{3/2}$	−0.05	−0.04	−0.03
	$5d_{5/2}$	0.08	0.06	0.06
83	$4s$	1.37	2.08	2.09
	$5s$	1.34	2.05	2.06
	$5p_{1/2}$	0.21	0.29	0.30
	$5p_{3/2}$	0.30	0.33	0.33
	$5d_{3/2}$	−0.04	−0.03	−0.02
	$5d_{5/2}$	0.09	0.07	0.07
92	$4s$	1.44	2.15	2.16
	$5s$	1.40	2.10	2.12
	$5p_{1/2}$	0.29	0.40	0.41
	$5p_{3/2}$	0.32	0.36	0.36
	$5d_{3/2}$	−0.03	−0.02	−0.01
	$5d_{5/2}$	0.09	0.08	0.07

calculations with H-like ions (see the next section) as well as for extending the active space of the model SE operator.

To obtain the function $F_{ik}(\alpha Z)$ for values of Z not listed in the tables, one may use a polynomial interpolation, applied to the function

$$G_{ik}(\alpha Z) = F_{ik}(\alpha Z) - \delta_{l0}(4/3)\ln(\alpha Z)^{-2}\,. \tag{25}$$

Here, following to Ref. [53], we have subtracted the log term which represents the small-αZ behavior of $F_{ik}(\alpha Z)$ for s states ($l = 0$). The interpolation function is thus given by [53]

$$F'_{ik}(\alpha Z) = \delta_{l0}(4/3)\ln(\alpha Z)^{-2} + \sum_{n=1}^{N}\left[\prod_{m\neq n}\frac{Z - Z_m}{Z_n - Z_m}\right] \times[F_{ik}(\alpha Z_n) - \delta_{l0}(4/3)\ln(\alpha Z_n)^{-2}]\,. \tag{26}$$

TABLE VII. The self-energy function $F(\alpha Z)$, defined by $\Delta E^{\rm SE} = \frac{\alpha}{\pi}\frac{(\alpha Z)^4}{n^3}F(\alpha Z)mc^2$, for neutral alkali metals in different potentials. $\langle v|h^{\rm SE}|v\rangle$ denotes the results of the model operator approach, calculated by averaging the model SE operator with the valence electron wave function in the corresponding potential. $\langle v|V^{\rm SE}_{\rm loc}|v\rangle$ is the contribution of the local part of the model SE operator, and "Exact" labels the results of the exact calculation of Ref. [20].

Atom	Method	$x_\alpha = 0$	$x_\alpha = 1/3$	$x_\alpha = 2/3$	$x_\alpha = 1$
Na $3s_{1/2}$	$\langle v\|V^{\rm SE}_{\rm loc}\|v\rangle$	0.166	0.163	0.176	0.214
	$\langle v\|h^{\rm SE}\|v\rangle$	0.170	0.168	0.183	0.224
	Exact [20]	0.169	0.167	0.181	0.223
K $4s_{1/2}$	$\langle v\|V^{\rm SE}_{\rm loc}\|v\rangle$	0.067	0.067	0.076	0.100
	$\langle v\|h^{\rm SE}\|v\rangle$	0.072	0.072	0.083	0.110
	Exact [20]	0.072	0.072	0.083	0.110
Rb $5s_{1/2}$	$\langle v\|V^{\rm SE}_{\rm loc}\|v\rangle$	0.0187	0.0193	0.0230	0.0320
	$\langle v\|h^{\rm SE}\|v\rangle$	0.0229	0.0237	0.0284	0.0397
	Exact [20]	0.0228	0.0236	0.0283	0.0396
Cs $6s_{1/2}$	$\langle v\|V^{\rm SE}_{\rm loc}\|v\rangle$	0.0093	0.0097	0.0118	0.0171
	$\langle v\|h^{\rm SE}\|v\rangle$	0.0127	0.0132	0.0163	0.0236
	Exact [20]	0.0126	0.0132	0.0162	0.0235
Fr $7s_{1/2}$	$\langle v\|V^{\rm SE}_{\rm loc}\|v\rangle$	0.0047	0.0052	0.0067	0.0102
	$\langle v\|h^{\rm SE}\|v\rangle$	0.0069	0.0076	0.0099	0.0151
	Exact [20]	0.0068	0.0075	0.0098	0.0150

V. CALCULATIONS WITH THE MODEL SELF-ENERGY OPERATOR

Since the model SE operator is constructed using the SE matrix elements with H-like wave functions of the ns states at $n \leqslant 3$ and the np and nd states at $n \leqslant 4$, first of all, we should consider how it works for H-like states with higher values of n. In Table VI we present the SE shifts for the $4s$, $5s$, $5p_{1/2}$, $5p_{3/2}$, $5d_{3/2}$, and $5d_{5/2}$ states in H-like ions, obtained using the model SE operator $\langle v|h^{\rm SE}|v\rangle$ and compare them with the corresponding exact results. To demonstrate the importance of the nonlocal part of $h^{\rm SE}$, we present also the local $\langle v|V^{\rm SE}_{\rm loc}|v\rangle$ contribution. As one can see from Table VI, for the s states the difference between the exact and model SE operator results does not exceed 1%. As for the p and d states, although the relative value of the difference is significantly bigger than for the s states, its absolute value, expressed in terms of the functions $F(\alpha Z)$, does not exceed 0.01. We stress also the importance of the nonlocal part of the model SE operator: for the s states the difference between the local part and the total result can amount to about 30%.

To demonstrate the efficiency of the method, we also applied it to calculations of the Lamb shifts in neutral alkali metals, Cu-like ions, superheavy atoms, and Li-like ions.

Calculations of the Lamb shift in alkali metals were considered in Refs. [20,54]. In Ref. [20], it was calculated in the potential $V_{\rm eff}(r)$, which is defined in terms of an effective charge $Z_{\rm eff}(r)$ through

$$V_{\rm eff}(r) = -\frac{\alpha Z_{\rm eff}(r)}{r}\,, \tag{27}$$

TABLE VIII. The self-energy contribution to the $4s$-$4p_{1/2}$, $4s$-$4p_{3/2}$, $4p_{1/2}$-$4d_{3/2}$, $4p_{3/2}$-$4d_{3/2}$, and $4p_{3/2}$-$4d_{5/2}$ transition energies in Cu-like ions (in eV). $\langle v|h^{\rm SE}|v\rangle$ denotes the results of the model operator approach, calculated by averaging the model SE operator with the Dirac-Kohn-Sham wave function of the valence electron. "Exact" labels the results of the exact calculation of Ref. [24].

Ion	Transition	$\langle v\|h^{\rm SE}\|v\rangle$	Exact [24]
Yb^{41+}	$4s$-$4p_{1/2}$	−1.29	−1.28
	$4s$-$4p_{3/2}$	−1.21	−1.21
	$4p_{1/2}$-$4d_{3/2}$	−0.10	−0.11
	$4p_{3/2}$-$4d_{3/2}$	−0.18	−0.18
	$4p_{3/2}$-$4d_{5/2}$	−0.14	−0.14
W^{45+}	$4s$-$4p_{1/2}$	−1.64	−1.64
	$4s$-$4p_{3/2}$	−1.55	−1.56
	$4p_{1/2}$-$4d_{3/2}$	−0.16	−0.17
	$4p_{3/2}$-$4d_{3/2}$	−0.25	−0.25
	$4p_{3/2}$-$4d_{5/2}$	−0.19	−0.19
Os^{47+}	$4s$-$4p_{1/2}$	−1.85	−1.84
	$4s$-$4p_{3/2}$	−1.75	−1.76
	$4p_{1/2}$-$4d_{3/2}$	−0.19	−0.20
	$4p_{3/2}$-$4d_{3/2}$	−0.28	−0.28
	$4p_{3/2}$-$4d_{5/2}$	−0.22	−0.22
Au^{50+}	$4s$-$4p_{1/2}$	−2.18	−2.18
	$4s$-$4p_{3/2}$	−2.10	−2.10
	$4p_{1/2}$-$4d_{3/2}$	−0.26	−0.28
	$4p_{3/2}$-$4d_{3/2}$	−0.35	−0.35
	$4p_{3/2}$-$4d_{5/2}$	−0.27	−0.28
Pb^{53+}	$4s$-$4p_{1/2}$	−2.57	−2.56
	$4s$-$4p_{3/2}$	−2.49	−2.50
	$4p_{1/2}$-$4d_{3/2}$	−0.35	−0.37
	$4p_{3/2}$-$4d_{3/2}$	−0.43	−0.43
	$4p_{3/2}$-$4d_{5/2}$	−0.34	−0.34
Bi^{54+}	$4s$-$4p_{1/2}$	−2.71	−2.70
	$4s$-$4p_{3/2}$	−2.64	−2.64
	$4p_{1/2}$-$4d_{3/2}$	−0.39	−0.40
	$4p_{3/2}$-$4d_{3/2}$	−0.46	−0.46
	$4p_{3/2}$-$4d_{5/2}$	−0.36	−0.37
Th^{61+}	$4s$-$4p_{1/2}$	−3.85	−3.85
	$4s$-$4p_{3/2}$	−3.88	−3.89
	$4p_{1/2}$-$4d_{3/2}$	−0.73	−0.74
	$4p_{3/2}$-$4d_{3/2}$	−0.70	−0.71
	$4p_{3/2}$-$4d_{5/2}$	−0.56	−0.57
U^{63+}	$4s$-$4p_{1/2}$	−4.24	−4.24
	$4s$-$4p_{3/2}$	−4.32	−4.33
	$4p_{1/2}$-$4d_{3/2}$	−0.87	−0.88
	$4p_{3/2}$-$4d_{3/2}$	−0.79	−0.79
	$4p_{3/2}$-$4d_{5/2}$	−0.63	−0.65

TABLE IX. The self-energy contribution to the binding energy of the valence electrons in Rg, Cn, E119 and E120 (in eV). In this work, the perturbation theory (PT) value is obtained by averaging the model SE operator with the Dirac-Fock wave function of the valence electron, while the DF and total DF values are obtained by including this operator in the DF equations. The DF value is given by the SE contribution to the one-electron binding energy, whereas the total DF value is obtained as the difference between the SE contributions to the total DF energies of the atom and the ion (the $^2S_{1/2} \to {}^1S_0$ and the $^1S_0 \to {}^2S_{1/2}$ transitions are considered for Rg and Cn, respectively; see the text). In Refs. [54,56], the calculations were performed with a local DF potential.

Atom	Valence electron	Method	This work	Ref. [56]	Other works
Rg	$7s$	PT	−0.088	−0.089	−0.087[a]
		DF	−0.105	−0.102	
		Total DF	−0.096		
		Welton method			−0.084[b]
		Local SE pot.			−0.089[c]
Cn	$7s$	PT	−0.101	−0.103	
		DF	−0.105	−0.110	
		Total DF	−0.098		
		Local SE pot.			−0.091[c]
E119	$8s$	PT	−0.0233		−0.0274[a]
		DF	−0.0250		
		Total DF	−0.0232		
		Local SE pot.			−0.0210[c]
E120	$8s$	PT	−0.0331		
		DF	−0.0265		
		Total DF	−0.0250		
		Local SE pot.			−0.0226[c]

[a] Taken from Ref. [54].
[b] Taken from Ref. [55].
[c] Taken from Ref. [31].

where

$$Z_{\rm eff}(r) = Z_{\rm nuc}(r) - r\int_0^\infty dr'\,\frac{1}{r_>}\rho_{\rm t}(r') + x_\alpha\left[\frac{81}{32\pi^2}r\rho_{\rm t}\right]^{1/3} \qquad (28)$$

and $\rho_{\rm t} = \rho_{\rm v} + \rho_{\rm c}$ is total (valence plus core) electron charge density, which is determined by self-consistently solving the Dirac equation with the potential $V_{\rm eff}(r)$ (see Ref. [20] for details). The choice $x_\alpha = 0$ corresponds to the Dirac-Hartree potential, $x_\alpha = 2/3$ gives the Kohn-Sham (KS) potential, and $x_\alpha = 1$ is the Dirac-Slater potential. In Table VII, we present the results of our calculations of the SE contribution to the Lamb shift performed for $x_\alpha = 0, 1/3, 2/3, 1$ and related exact data by Sapirstein and Cheng [20]. Our data were obtained by averaging the model SE operator $h^{\rm SE}$, given by Eq. (22), with the wave function of the valence state v determined from the Dirac equation with the potential $V_{\rm eff}(r)$. To demonstrate the importance of the nonlocal part of $h^{\rm SE}$, in addition to the total $\langle v|h^{\rm SE}|v\rangle$ contribution, we present also the local $\langle v|V^{\rm SE}_{\rm loc}|v\rangle$ part. As one can see from the Table VII, for all atoms the $\langle v|h^{\rm SE}|v\rangle$ values are in a good agreement with the exact results, while the local potential approximation $\langle v|V^{\rm SE}_{\rm loc}|v\rangle$ works reasonably well only for low-Z systems.

In Ref. [24], the QED corrections to the transition energies in Cu-like ions have been calculated in the Kohn-Sham potential. In Table VIII, we present the SE corrections to the $4s$-$4p_{1/2}$, $4s$-$4p_{3/2}$, $4p_{1/2}$-$4d_{3/2}$, $4p_{3/2}$-$4d_{3/2}$, and $4p_{3/2}$-$4d_{5/2}$ transition energies obtained by averaging the model SE operator with the wave function of the valence electron. This wave function was calculated by solving the KS equation with the KS potential constructed self-consistently with the

TABLE X. The screened self-energy for the $2s$, $2p_{1/2}$, and $2p_{3/2}$ states of Li-like ions (in eV). The Kohn-Sham (KS) and Dirac-Fock (DF) results are obtained by calculating the total ion energy with the model SE operator included in the KS and DF equations, respectively, and subtracting the related energies evaluated without the model SE operator and the self-energy contributions calculated with the hydrogenlike wave functions. A comparison with the calculations performed by perturbation theory (PT) in the Kohn-Sham potential [26,27] is given.

Z	State	KS	DF	PT [26]	PT [27]
20	$2s$	−0.047	−0.045	−0.044	−0.046
	$2p_{1/2}$	−0.009	−0.008	−0.008	−0.008
	$2p_{3/2}$	−0.012	−0.011	−0.013	−0.013
40	$2s$	−0.277	−0.269		−0.260
	$2p_{1/2}$	−0.063	−0.059		−0.059
	$2p_{3/2}$	−0.077	−0.073		−0.085
50	$2s$	−0.50	−0.49	−0.48	
	$2p_{1/2}$	−0.13	−0.12	−0.12	
	$2p_{3/2}$	−0.14	−0.14	−0.16	
60	$2s$	−0.84	−0.82		−0.80
	$2p_{1/2}$	−0.24	−0.24		−0.25
	$2p_{3/2}$	−0.24	−0.23		−0.27
74	$2s$	−1.58	−1.55		−1.55
	$2p_{1/2}$	−0.57	−0.56		−0.62
	$2p_{3/2}$	−0.45	−0.43		−0.53
83	$2s$	−2.35	−2.25	−2.32	−2.26
	$2p_{1/2}$	−0.97	−0.98	−1.07	−1.07
	$2p_{3/2}$	−0.65	−0.61	−0.75	−0.76
92	$2s$	−3.47	−3.19		−3.81
	$2p_{1/2}$	−1.67	−1.69		−1.58
	$2p_{3/2}$	−0.91	−0.86		−1.04

$4s$ state. The comparison with the related exact results from Ref. [24] is also given. It can be seen that the model SE operator results are in a very good agreement with the exact results.

Experiments with superheavy elements have triggered a great interest in calculations of the QED effects in superheavy atoms [31,32,54–56]. In Ref. [56], the QED contributions to the binding energy of the valence $7s$ electrons in Rg ($Z = 111$) and Cn ($Z = 112$) have been evaluated in a local Dirac-Fock potential. In Table IX, we compare the related SE contributions obtained using the model SE operator in the Dirac-Fock method with those by Goidenko [56]. Although the calculations in the local DF potential are not fully equivalent to the calculations based on the DF equations, the SE contributions to the one-electron binding energies obtained by averaging the model SE operator with the DF wave function of the valence electron as well as by including this operator in the DF equations are in good agreement with Goidenko's corresponding results. For comparison, we present also the total DF values, which are obtained as the difference between the SE contributions to the total DF energies of the atom and the ion. It is known [57,58] that for Rg and Cn the ionization occurs out of the $6d_{5/2}$ shell instead of the $7s$ shell. However, for comparison purposes, here we consider the ${}^2S_{1/2} \to {}^1S_0$ transition for Rg and the ${}^1S_0 \to {}^2S_{1/2}$ transition for Cn. The presented results are also in reasonable agreement with those based on the Welton method [55] and with the results obtained using a local SE potential [31]. In Table IX, we give also the results of our calculations of the SE corrections to the binding energy of the valence $8s$ electrons in E119 and E120 and compare them with the values obtained in Ref. [31].

Finally, we applied our model approach to the Li-like ions, for which rigorous QED calculations have been performed. The self-energy screening diagrams for Li-like ions to first order in $1/Z$ were first evaluated in Ref. [15]. In that paper, the calculations were performed in the Coulomb potential. Later, the same diagrams were calculated in the Kohn-Sham and core-Hartree potentials [26,27]. In Table X, we present the results of our calculations of the screened SE corrections in Li-like ions based on the model SE operator approach and compare them with the related results from Refs. [26,27]. In our approach, the screened SE corrections were obtained by calculating the total ion energy with the model SE operator included in the DF or the KS equation and subtracting both the related energy evaluated without the model SE operator and the SE contribution evaluated with the H-like wave functions. In the case of the KS method, the KS potential was constructed self-consistently with the valence state under consideration. As one can see from Table X, the model SE operator results obtained employing the KS and DF equations are in fair agreement with the results obtained with the perturbation theory [26,27]. Therefore, to good accuracy, the total SE corrections can be obtained by summing the H-like SE contributions and the screened SE corrections evaluated by solving either DF or KS equations with the model SE operator included, as described above.

VI. CONCLUSION

In this paper we have developed the model QED operator approach to calculations of the Lamb shifts in relativistic atomic systems. With this method, we proposed the model self-energy operator which is given by Eq. (22). This operator can be easily incorporated in any calculations employing the Dirac-Coulomb-Breit Hamiltonian. This was demonstrated by calculating the Lamb shifts in atoms and ions with the use of the model SE operator and comparing the obtained results with corresponding exact QED calculations.

ACKNOWLEDGMENTS

We thank Andrey Volotka for providing us with details of his calculations of the self-energy screening diagrams performed in Ref. [26]. Valuable discussions with Jan Derezinski, Bogumil Jeziorski, and Jonathan Sapirstein are gratefully acknowledged. This work was supported by RFBR (Grants No. 13-02-00630 and No. 11-02-00943-a) and by the Ministry of Education and Science of the Russian Federation (Grant No. 8420).

[1] I. P. Grant, Adv. Phys. **19**, 747 (1970).

[2] J. P. Desclaux, Comput. Phys. Commun. **9**, 31 (1975).

[3] V. F. Bratsev, G. B. Deyneka, and I. I. Tupitsyn, Bull. Acad. Sci. USSR Phys. Ser. **41**, 173 (1977).

[4] P. Indelicato and J. P. Desclaux, Phys. Rev. A **42**, 5139 (1990).

[5] M. G. Kozlov, S. G. Porsev, and I. I. Tupitsyn, Phys. Rev. Lett. **86**, 3260 (2001).

[6] D. A. Glazov, V. M. Shabaev, I. I. Tupitsyn, A. V. Volotka, V. A. Yerokhin, G. Plunien, and G. Soff, Phys. Rev. A **70**, 062104 (2004).

[7] I. I. Tupitsyn, A. V. Volotka, D. A. Glazov, V. M. Shabaev, G. Plunien, J. R. Crespo Lopez-Urrutia, A. Lapierre, and J. Ullrich, Phys. Rev. A **72**, 062503 (2005).

[8] V. A. Dzuba, V. V. Flambaum, and O. P. Sushkov, Phys. Lett. A **141**, 147 (1989).

[9] S. A. Blundell, W. R. Johnson, and J. Sapirstein, Phys. Rev. Lett. **65**, 1411 (1990); S. A. Blundell, J. Sapirstein, and W. R. Johnson, Phys. Rev. D **45**, 1602 (1992).

[10] P. Indelicato and E. Lindroth, Phys. Rev. A **46**, 2426 (1992).

[11] A. Ynnerman, J. James, I. Lindgren, H. Persson, and S. Salomonson, Phys. Rev. A **50**, 4671 (1994).

[12] M. S. Safronova, W. R. Johnson, and A. Derevianko, Phys. Rev. A **60**, 4476 (1999).

[13] S. G. Porsev, K. Beloy, and A. Derevianko, Phys. Rev. Lett. **102**, 181601 (2009); Phys. Rev. D **82**, 036008 (2010).

[14] V. A. Dzuba, J. C. Berengut, V. V. Flambaum, and B. Roberts, Phys. Rev. Lett. **109**, 203003 (2012).

[15] V. A. Yerokhin, A. N. Artemyev, T. Beier, G. Plunien, V. M. Shabaev, and G. Soff, Phys. Rev. A **60**, 3522 (1999).

[16] A. N. Artemyev, V. M. Shabaev, V. A. Yerokhin, G. Plunien, and G. Soff, Phys. Rev. A **71**, 062104 (2005).

[17] V. M. Shabaev, Phys. Usp. **51**, 1175 (2008).

[18] D. A. Glazov, Y. S. Kozhedub, A. V. Maiorova, V. M. Shabaev, I. I. Tupitsyn, A. V. Volotka, C. Kozhuharov, G. Plunien, and Th. Stóhlker, Hyperfine Interact. **199**, 71 (2011).

[19] A. V. Volotka, D. A. Glazov, O. V. Andreev, V. M. Shabaev, I. I. Tupitsyn, and G. Plunien, Phys. Rev. Lett. **108**, 073001 (2012).

[20] J. Sapirstein and K. T. Cheng, Phys. Rev. A **66**, 042501 (2002).

[21] J. Sapirstein and K. T. Cheng, Phys. Rev. A **68**, 042111 (2003).

[22] V. M. Shabaev, K. Pachucki, I. I. Tupitsyn, and V. A. Yerokhin, Phys. Rev. Lett. **94**, 213002 (2005).

[23] V. M. Shabaev, I. I. Tupitsyn, K. Pachucki, G. Plunien, and V. A. Yerokhin, Phys. Rev. A **72**, 062105 (2005).

[24] M. H. Chen, K. T. Cheng, W. R. Johnson, and J. Sapirstein, Phys. Rev. A **74**, 042510 (2006).

[25] A. N. Artemyev, V. M. Shabaev, I. I. Tupitsyn, G. Plunien, and V. A. Yerokhin, Phys. Rev. Lett. **98**, 173004 (2007).

[26] Y. S. Kozhedub, A. V. Volotka, A. N. Artemyev, D. A. Glazov, G. Plunien, V. M. Shabaev, I. I. Tupitsyn, and Th. Stöhlker, Phys. Rev. A **81**, 042513 (2010).

[27] J. Sapirstein and K. T. Cheng, Phys. Rev. A **83**, 012504 (2011).

[28] P. Pyykko and L.-B. Zhao, J. Phys. B **36**, 1469 (2003).

[29] I. Draganic, J. R. Crespo López-Urrutia, R. DuBois, S. Fritzsche, V. M. Shabaev, R. S. Orts, I. I. Tupitsyn, Y. Zou, and J. Ullrich, Phys. Rev. Lett. **91**, 183001 (2003).

[30] V. V. Flambaum and J. S. M. Ginges, Phys. Rev. A **72**, 052115 (2005).

[31] C. Thierfelder and P. Schwerdtfeger, Phys. Rev. A **82**, 062503 (2010).

[32] P. Pyykko, Chem. Rev. **112**, 371 (2012).

[33] I. I. Tupitsyn and E. V. Berseneva, Opt. Spectrosc. **114**, 682 (2013).

[34] J. A. Lowe, C. T. Chantler, and I. P. Grant, Radiat. Phys. Chem. **85**, 118 (2013).

[35] B. M. Roberts, V. A. Dzuba, and V. V. Flambaum, Phys. Rev. A **87**, 054502 (2013).

[36] T. A. Welton, Phys. Rev. **74**, 1157 (1948).

[37] V. M. Shabaev, J. Phys. B **26**, 4703 (1993).

[38] V. M. Shabaev, Phys. Rep. **356**, 119 (2002).

[39] M. H. Mittleman, Phys. Rev. A **5**, 2395 (1972).

[40] J. Sucher, Phys. Rev. A **22**, 348 (1980).

[41] P. J. Mohr, G. Plunien, and G. Soff, Phys. Rep. **293**, 227 (1998).

[42] L. W. Fullerton and G. A. Rinker, Jr., Phys. Rev. A **13**, 1283 (1976).

[43] G. Soff and P. J. Mohr, Phys. Rev. A **38**, 5066 (1988).

[44] N. L. Manakov, A. A. Nekipelov, and A. G. Fainshtein, Sov. Phys. JETP **68**, 673 (1989).

[45] H. Persson, I. Lindgren, S. Salomonson, and P. Sunnergren, Phys. Rev. A **48**, 2772 (1993).

[46] A. G. Fainshtein, N. L. Manakov, and A. A. Nekipelov, J. Phys. B **24**, 559 (1991).

[47] P. J. Mohr, Phys. Rev. A **46**, 4421 (1992).

[48] P. J. Mohr and Y.-K. Kim, Phys. Rev. A **45**, 2727 (1992).

[49] T. Beier, P. J. Mohr, H. Persson, and G. Soff, Phys. Rev. A **58**, 954 (1998).

[50] V. A. Yerokhin and V. M. Shabaev, Phys. Rev. A **60**, 800 (1999).

[51] V. A. Yerokhin, K. Pachucki, and V. M. Shabaev, Phys. Rev. A **72**, 042502 (2005).

[52] V. A. Yerokhin, Phys. Rev. A **83**, 012507 (2011).

[53] P. J. Mohr, At. Data Nucl. Data Tables **29**, 453 (1983).

[54] L. Labzowsky, I. Goidenko, M. Tokman, and P. Pyykko, Phys. Rev. A **59**, 2707 (1999).

[55] P. Indelicato, J. P. Santos, S. Boucard, and J.-P. Desclaux, Eur. Phys. J. D **45**, 155 (2007).

[56] I. A. Goidenko, Eur. Phys. J. D **55**, 35 (2009).

[57] E. Eliav, U. Kaldor, P. Schwerdtfeger, B. A. Hess, and Y. Ishikawa, Phys. Rev. Lett. **73**, 3203 (1994).

[58] E. Eliav, U. Kaldor, and Y. Ishikawa, Phys. Rev. A **52**, 2765 (1995).